# Coagulation Factor XIII-A Subunit Missense Mutation in the Pathobiology of Autosomal Dominant Multiple Dermatofibromas

Chavalit Supsrisunjai[1,2], Chao-Kai Hsu[1,3,4], Magdalene Michael[5], Cédric Duval[6], John Y.W. Lee[1], Hsing-San Yang[3], Hsin-Yu Huang[7], Thitiwat Chaikul[1], Alexandros Onoufriadis[1], Roberto A. Steiner[5], Robert A.S. Ariëns[6], Ofer Sarig[8], Eli Sprecher[8,9], Marina Eskin-Schwartz[8], Curt Samlaska[10], Michael A. Simpson[11], Eduardo Calonje[1,12], Maddy Parsons[5] and John A. McGrath[1]

Dermatofibromas are common benign skin lesions, the etiology of which is poorly understood. We identified two unrelated pedigrees in which there was autosomal dominant transmission of multiple dermatofibromas. Whole exome sequencing revealed a rare shared heterozygous missense variant in the *F13A1* gene encoding factor XIII subunit A (FXIII-A), a transglutaminase involved in hemostasis, wound healing, tumor growth, and apoptosis. The variant (p.Lys679Met) has an allele frequency of 0.0002 and is predicted to be a damaging mutation. Recombinant human Lys679Met FXIII-A demonstrated reduced fibrin crosslinking activity in vitro. Of note, the treatment of fibroblasts with media containing Lys679Met FXIII-A led to enhanced adhesion, proliferation, and type I collagen synthesis. Immunostaining revealed co-localization between FXIII-A and α4β1 integrins, more prominently for Lys679Met FXIII-A than the wild type. In addition, both the α4β1 inhibitors and the mutation of the FXIII-A Isoleucine-Leucine-Aspartate-Threonine (ILDT) motif prevented Lys679Met FXIII-A-dependent proliferation and collagen synthesis of fibroblasts. Our data suggest that the Lys679Met mutation may lead to a conformational change in the FXIII-A protein that enhances α4-integrin binding and provides insight into an unexpected role for FXIII-A in the pathobiology of familial dermatofibroma.

*Journal of Investigative Dermatology* (2020) **140,** 624–635; doi:10.1016/j.jid.2019.08.441

## INTRODUCTION

Dermatofibromas are common benign fibro-histiocytic tumors (Jakobiec et al., 2017, 2014). Typically, dermatofibromas present as solitary 0.5 to 1 cm pink, red, tan, or flesh-colored lumps with an overlying dimple-like depression (Zelger and Zelger, 1998). Sometimes multiple dermatofibromas may occur, occasionally in families but more often in individuals with underlying immunologic or other clinical abnormalities (Beatrous et al., 2017). The most common site for dermatofibromas is the lower leg, with the usual onset during early adulthood. The cause of dermatofibromas is not known, although dermatologists may suggest that they occur following insect bites in susceptible individuals, or possibly following trauma (Kluger et al., 2008; Myers and Fillman, 2019).

Histologically, in dermatofibromas (single or multiple), there are interlacing fascicles of slender spindle-shaped cells within a loose collagenous, or occasionally myxoid, stroma. Of note, hemosiderin is frequently present. Immunohistochemically, almost all dermatofibromas are factor XIIIA antigen-positive (Altman et al., 1993), and indeed, immunostaining for FXIII-A is frequently used in the tissue diagnosis of dermatofibromas (Cerio et al., 1988, 1989).

In this study, we performed whole exome sequencing to identify the causative mutation in two seemingly unrelated pedigrees with autosomal dominant familial multiple dermatofibromas. Intriguingly, we identified the same mutation in *F13A1* encoding the A-subunit of factor XIII (FXIII-A) in both families. FXIII is a member of the transglutaminase family, which crosslinks various proteins involved in hemostasis, wound healing, tumor growth, and apoptosis (Muszbek et al., 2011). During wound healing, FXIII modulates fibroblast and macrophage biology and contributes to angiogenesis (Bagoly et al., 2012; Duval et al., 2016; Muszbek et al., 2011). While plasma FXIII is composed of

[1]*St John's Institute of Dermatology, School of Basic and Medical Biosciences, King's College London, Guy's Hospital, London, United Kingdom;* [2]*Institute of Dermatology, Ministry of Public Health, Bangkok, Thailand;* [3]*Department of Dermatology, National Cheng Kung University Hospital, College of Medicine, National Cheng Kung University, Tainan, Taiwan;* [4]*International Center for Wound Repair and Regeneration, National Cheng Kung University, Tainan, Taiwan;* [5]*Randall Centre for Cell and Molecular Biophysics, School of Basic and Medical Biosciences, King's College London, United Kingdom;* [6]*Leeds Institute of Cardiovascular and Metabolic Medicine, University of Leeds, Leeds, United Kingdom;* [7]*School of Medicine, College of Medicine, National Cheng Kung University, Tainan, Taiwan;* [8]*Division of Dermatology, Tel Aviv Sourasky Medical Center, Tel Aviv, Israel;* [9]*Department of Human Molecular Genetics & Biochemistry, Sackler Faculty of Medicine, Tel-Aviv University, Tel-Aviv, Israel;* [10]*Academic Dermatology of Nevada, University of Nevada School of Medicine, Reno, Nevada;* [11]*Department of Genetics, School of Basic and Medical Biosciences, King's College London, Guy's Hospital, London, United Kingdom; and* [12]*Department of Dermatopathology, St John's Institute of Dermatology, Guy's and St Thomas' NHS Foundation Trust, London, United Kingdom*

*Correspondence: John McGrath, Dermatology Research Labs, Floor 9 Tower Wing, Guy's Hospital, Great Maze Pond, London SE1 9RT, United Kingdom. E-mail: john.mcgrath@kcl.ac.uk*

*Abbreviations: Akt, protein kinase B; CDM, cell-derived matrix; FXIII-A, factor XIII subunit A; HEK, human embryonic kidney; ILDT, Isoleucine-Leucine-Aspartate-Threonine; TBS, tris buffered saline; WT, wild type*

*Received 1 July 2019; revised 26 July 2019; accepted 6 August 2019; accepted manuscript published online 4 September 2019; corrected proof published online 27 November 2019*

two catalytic A subunits and two non-catalytic carrier B units that generate an $A_2B_2$ heterotetramer (Komáromi et al., 2011), cellular FXIII (found, for example, in platelets and megakaryocytes) is formed solely of A subunits organized in an $A_2$ homodimer. The mutation we identified in this study affects the A subunit, that is, it impacts on both the plasma and tissue and cellular FXIII forms (PMID: 30489000, PMID: 5096097). We provide evidence that the FXIII-A mutation leads to enhanced proliferation and collagen synthesis in fibroblasts, potentially through promotion of the binding of exogenous FXIII-A to integrins. Our study therefore provides insight into an important role for FXIII-A in the etiology and pathobiology of some dermatofibromas.

## RESULTS

### Clinical features and histology

We examined seven affected individuals from two unrelated families with multiple dermatofibromas inherited in an autosomal dominant pattern (Figure 1a). Three affected individuals were from the Ukraine (family 1), and four affected were from the USA (family 2). Both families were Jewish (Ashkenazi). Some clinicopathologic details of family 2 have been published previously (Samlaska and Bennion, 2002). All the subjects presented with multiple lesions of erythematous papules over their extremities (Figure 1b; illustrations from family 1 and 2) with histopathologic findings of dermatofibromas (Figure 1c; family 1, II-2). No extra-cutaneous manifestations were reported.

### All individuals with multiple dermatofibromas are heterozygous for the mutation c.2036A>T (Lys679Met) in *F13A1*

We undertook whole exome sequencing in six affected subjects from the Ukraine and US families and two unaffected individuals from the US family. Candidate mutations were prioritized by filtering for variants with a frequency of less than 0.01% in public repositories, such as the 1000 Genomes Project, Exome Aggregation Consortium, and an in-house database (Supplementary Tables S1 and S2). Using these criteria, a missense variant in *F13A1* encoding Factor XIII subunit A (c.2036A>T; rs201302247) was the only variant present in all the affected individuals in both families. Subsequent Sanger sequencing confirmed the mutation in affected individuals (Supplementary Figure S1) and indicated that it co-segregated with disease status in all the relatives who provided DNA samples. This variant was rare in the population (less than 0.0207% frequency) and resulted in an amino acid change from lysine to methionine at position 679 (position 678 in the mature protein) with an in silico prediction that the mutation is damaging (Polyphen-2 = 1; Mutation taster = 1; CADD = 25.5; DANN = 0.993).

### c.2036A>T in *F13A1* is a rare allele most commonly found in Ashkenazi Jews

To investigate the possibility that c.2036A>T was inherited from a common ancestor, we performed a haplotype analysis to study the mutant alleles from affected individuals using four highly polymorphic single nucleotides polymorphism markers based on the exome data (Supplementary Figure S2). The data showed identical haplotypes among the affected individuals (in contrast to the unaffected individuals) indicating that c.2036A>T probably occurred on the same ancestral allele. Of note, the allele frequency of rs201302247 in Ashkenazi Jews (0.397%) is almost 20 times higher than that in the general population (Genome Aggregation Database; https://gnomad.broadinstitute.org/variant/6-6152055-T-A). The incidence of familial multiple dermatofibromas is not known (in any population), but our data indicate that, although rare and perhaps underreported, it may be substantially higher in Ashkenazi Jews.

### Mutations in *F13A1* are not detectable in sporadic dermatofibromas

To explore whether mutations in *F13A1* might also be present in the more common sporadic dermatofibromas, we undertook Sanger sequencing of the coding and promoter regions of *F13A1* using DNA extracted from paraffin-embedded tissue of 22 sporadic single dermatofibromas from unrelated individuals; no potentially deleterious variants were identified (Supplementary Methods and Results, and Supplementary Tables S3–S6).

### The mutation Lys679Met in FXIII-A results in reduced crosslinking activity

To assess the activity of the Lys679Met mutant FXIII-A protein, we generated glutathione S-transferase-fusions of wild type (WT) or Lys679Met FXIII-A (see Supplementary Table S7 for site-directed mutagenesis details), purified recombinant proteins (Figure 2a), and performed pentylamine incorporation into casein assays. We found that the Lys679Met FXIII-A mutation led to reduced crosslinking at 30 minutes by 50% compared to the WT protein (Figure 2b and c). To find possible clues for the altered catalytic activity, we looked at the structural information available. FXIII-A is composed of five major structural regions: an N-terminal activation peptide (residues 1–38), a β-sandwich domain (residues 39–184), a catalytic domain (185–516), and two β-barrel domains (517–628 and 629–732) that in the inactive FXIII-A zymogen are arranged in a dimer (Figure 2d) (Yee et al., 1994; Weiss et al., 1998). Residue Lys679 is solvent-exposed and maps on a β-strand of the second β-barrel domain. In the inactive enzyme, access to the active site is occluded by an intramolecular interaction within the first β-barrel domain, which, in turn, is stabilized by the N-terminal peptide of the second FXIII-A molecule. Enzyme activation involves the thrombin cleavage of the activation peptide in the presence of $Ca^{2+}$ ions, and calcium binding results in dimer destabilization and a large structural rearrangement involving a swinging movement of both β-barrel domains (Figure 2e). This leads to an active FXIII-A monomer in which the active site is accessible (Stieler et al., 2013). In the active conformation observed by crystallography, Lys679 is located away from the active site (more than 6.3 nm), ruling out a direct effect of the Lys to Met mutation on the catalytic machinery. This mutation could alternatively play a role in the activation mechanism. The first five amino acids of the activation peptide are not visible in the structure of the inactive FXIII-A dimer, and Lys679 is approximately 2.2 nm away from the first ordered residue (Arg 6). Thus, based on distance considerations, stabilization of the flexible N-terminal

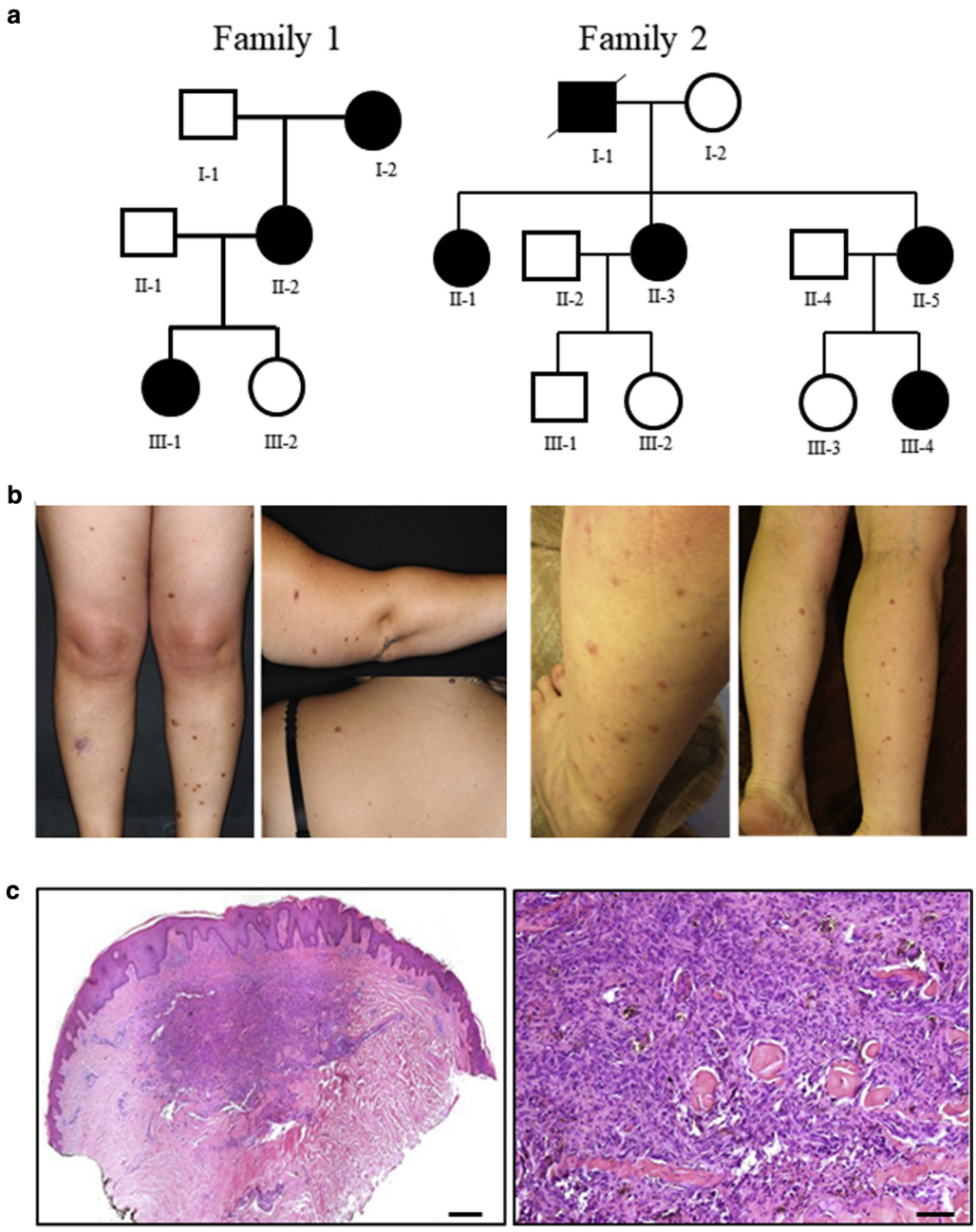


**Figure 1. Clinicopathologic and molecular basis of familial multiple dermatofibromas.** (**a**) Pedigrees of the two families showing all affected individuals with the *F13A1* mutation c.2036A>T (Lys679Met). (**b**) Multiple dermatofibromas in Family 1 individual II-2 (left) and Family 2 individuals II-3 (right). (**c**) Histopathologic features of an excised dermatofibromas from an individual II-2 in Family 1 showing the proliferation of fibro-histiocytic cells within the dermis with an overlying Grenz zone (left image; hematoxylin and eosin, ×4; Bar = 500 μm). There is collagen entrapment at the periphery of the lesion, as well as the presence of hemosiderin pigment (right image; hematoxylin and eosin, ×10; Bar = 200 μm).

peptide by the Lys679Met residue would require some structural rearrangements. We should also point out that in our pentylamine incorporation assay, we employed Prescission-cleaved recombinant FXIII-A. Therefore, we cannot exclude the possibility that the slightly longer N-terminus resulting from the cloning strategy fortuitously might be stabilized by the Lys679Met mutation more than occurs in vivo wherein the Ser2 is expected to be acetylated following cleavage of the first methionine (GPMSETSR…. instead of Ac-SETSR….). More detailed biochemical experiments need to be performed to validate the observed change in catalytic activity and understand its possible molecular basis.

### The mutation Lys679Met in FXIII-A promotes proliferation and collagen production in human dermal fibroblasts

Proliferation assays were performed to determine whether FXIII-A contributes to fibroblast cell proliferation in dermatofibromas. To expose fibroblasts to FXIII-A, we expressed WT or Lys679Met FXIII-A coupled to green fluorescent protein by means of an internal ribosome entry site in human embryonic kidney (HEK293) cells and collected secreted

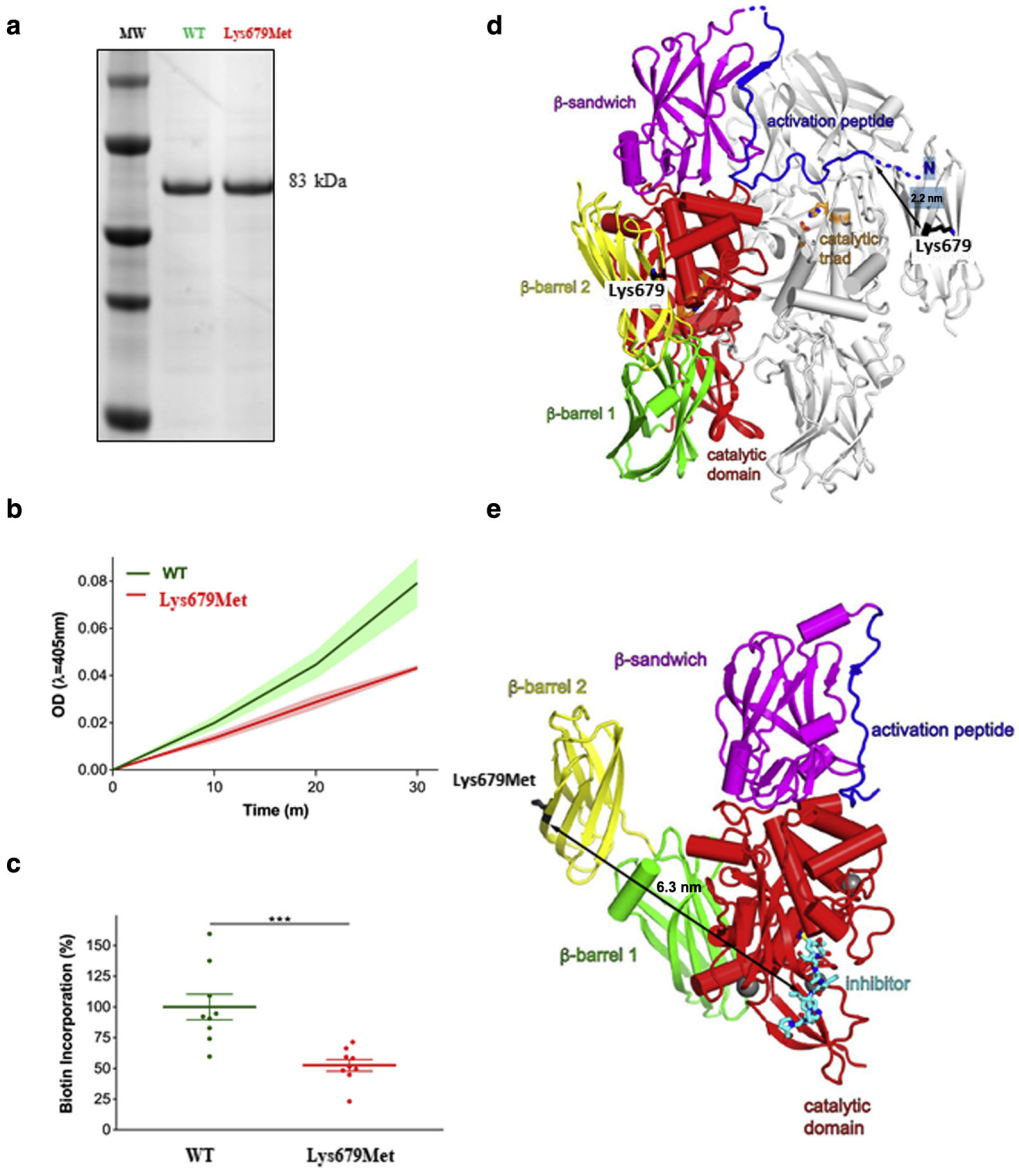


**Figure 2. Mutation Lys679Met in FXIII-A leads to reduced protein activity** (**a**) SDS-PAGE gel showing purity and levels of WT and Lys679Met FXIII-A purified recombinant proteins used in the assay. (**b**) Graph showing the rate of pentylamine incorporation over time in preparations containing WT or Lys679Met mutant protein. (**c**) Percentage biotin incorporation as an estimation of FXIII activity. The data display the means ± SD for three experiments. ***$P = 0.0007$. (**d**) Cartoon representation of the inactive FXIII-A dimer (PDB code 1F13). For one FXIII-A molecule, distinct structural regions are labeled and highlighted using different colors. The second FXIII-A molecule is shown in gray. The Lys679 residue is shown as a stick representation in black. Residues of the catalytic triad are shown in orange. Lys679 is located ~2.2 nm away from the first ordered residue of the N-terminal activation peptide. (**e**) Cartoon representation of the Ca2+-activated FXIII-A monomer (PDB code 4KTY) shown in the same orientation as in **d**. Color-codes for the distinct structural regions are the same as in **d**. The inhibitor bound in the active site is shown in cyan. Calcium ions are shown as gray spheres. Residue Lys679 is shown as stick representation in black. $Ca^{2+}$-induced activation elicits a large swinging movement of the β-barrel domains. In this conformation, Lys679 is located ~6.3 nm away from the active site. WT, wild type.

protein in the conditioned media. Both WT and Lys679Met constructs yielded similar levels of secreted protein (Figure 3a, inset blot). Treatment of fibroblasts with this media demonstrated that incubation with WT FXIII-A led to higher proliferation rates after 48 hours, whereas Lys679Met FXIII-A led to significantly higher proliferation rates at both 24 and 48 hours post-incubation (Figure 3a). To determine whether treatment with FXIII-A also altered pro-fibrotic matrix secretion by fibroblasts, collagen I and fibronectin levels were assessed in whole cell lysates. Western blots revealed a significant increase in collagen synthesis in Lys679Met FXIII-A treated cells but not those treated with WT FXIII-A media, compared with the controls (Figure 3b), whereas no change in the levels of fibronectin were detected between samples (Supplementary Figure S3a). Quantitative PCR analysis further demonstrated the upregulation of collagen I mRNA levels in Lys679Met FXIII-A treated cells compared to the WT (Figure 3c). To further analyze the native extracellular matrix deposition by cells, the fibroblasts were grown for 14 days on coverslips to generate cell-derived matrix (CDM) in the presence or absence of FXIII-A. Imaging of the resulting CDM preparations revealed an apparent

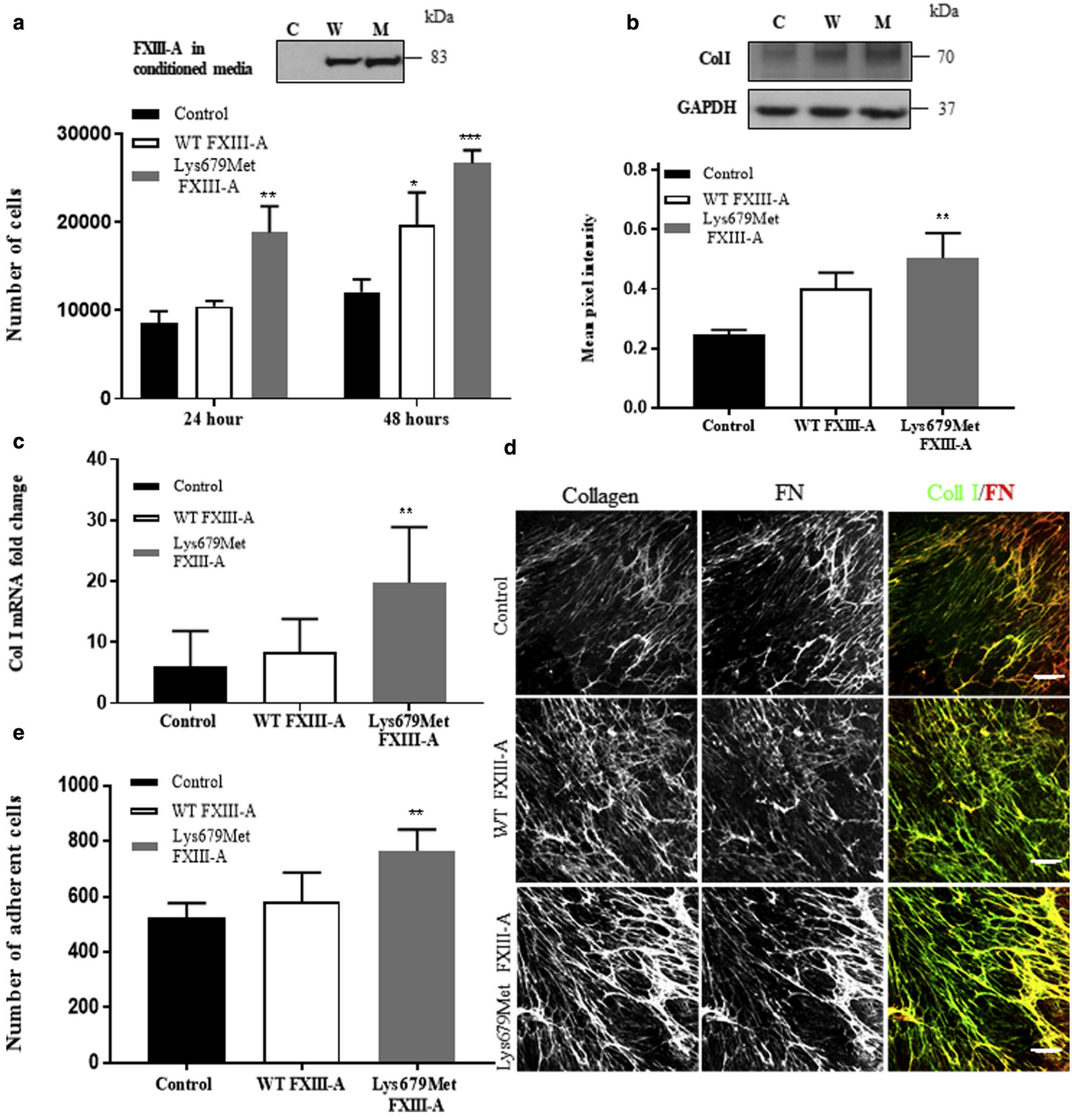


**Figure 3. Mutation of Lys679Met in FXIII-A leads to increased fibroblast proliferation, collagen production, and changes in extracellular matrix organization.** (**a**) Graph shows that NHDF proliferation is increased for Lys679Met FXIII-A compared to WT FXIII-A at both 24 and 48 hours. (**b**) Collagen I western blot and (**c**) qPCR show that Lys679Met FXIII-A promotes more collagen I production after 48 hours compared with WT FXIII-A. (**d**) Images of CDM produced by cells showing those treated with Lys679Met FXIII-A express more collagen made of thickened fibers compared to WT FXIII-A (Bar = 10 um). (**e**) Adhesion assay showing the number of cells adhering to the collagen I-coated plate at 1 hour is greater for Lys679Met FXIII-A compared with the WT FXIII-A. The data indicate the means ± SD for three experiments. $*P < 0.05$, $**P < 0.01$ vs control, $***P < 0.001$ vs control. All the experiments were done in triplicate (n = 3). C, control; FXIII-A, factor XIII subunit A; M, mutant; NHDF, normal human dermal fibroblast; qPCR, quantitative reverse transcriptase in real time; WT, wild type.

increase in disorganized collagen production in the cells treated with Lys679Met FXIII-A compared with those of the WT (Figure 3d). These combined data suggest that FXIII-A can promote fibroproliferative responses in fibroblasts and that the identified Lys679Met mutation enhances this property of FXIII-A.

### Lys679Met FXIII-A shows a higher association with α4β1 integrins on fibroblasts

Our data demonstrated that, in contrast to lower activity as a coagulation factor, Lys679Met FXIII-A exhibited more activity in terms of a fibroproliferation. Previous data have suggested that FXIII-A binds to α4β1 integrin to elicit some cellular

activities (Isobe et al., 1999). To explore this possibility, we performed early adhesion assays to collagen I substrates of fibroblasts pre-treated with WT or Lys679Met FXIII-A. The data revealed a significant increase in the adhesion of cells treated with Lys679Met FXIII-A compared with the WT or control samples (Figure 3e), suggesting enhanced integrin activation in these cells. Given that α4β1 integrin is a fibronectin receptor and does not directly bind to collagen I, other matrix receptors, for example, α1β1 or α2β1 integrin may be involved in the binding.

To investigate whether FXIII-A binds to specific sites on the cell surface, the localization patterns of FXIII-A, α4, and active β1 integrins were analyzed in FXIII-A-treated fibroblasts by confocal microscopy. Images and subsequent analysis revealed that active β1 integrins co-localized with WT FXIII-A, and this was significantly increased for Lys679-Met FXIII-A (Figure 4a and b). Moreover, levels of the active β1 integrins were significantly higher in Lys679Met FXIII-A treated cells compared to the WT or untreated cells (Figure 4c), further supporting the concept that mutant FXIII-A can activate integrin receptors at the surface of fibroblasts. Similarly, α4 integrins showed a significant increase in co-localization with Lys679Met FXIII-A compared to the WT (Figure 4d and e), indicating that mutant FXIII-A either binds with higher specificity to α4 integrin, or that the protein remains at these sites for longer after binding. No significant difference in the levels of total α4 integrin protein were observed between the WT- and Lys679Met FXIII-A-treated cells (Supplementary Figure S3c and d), suggesting that FXIII-A exerts its effects at the level of integrin localization in fibroblasts. This observation suggests that FXIII-A associates with integrins and results in increased receptor activation.

To further investigate whether FXIII-A may cooperate with α4β1 to elicit phenotypic effects, cells were pre-treated with α4β1-specific inhibitors (BIO1211, BOP [IUPAC name: N-(Benzenesulfonyl)-L-prolyl-L-(1-pyrrolidinylcarbonyl) tyrosine sodium salt], and TCS2134) before treatment with FXIII-A. Confocal imaging of α4β1 integrins revealed a visible reduction in the levels of both WT and Lys679Met FXIII-A associated with the plasma membrane in cells treated with BIO1211, suggesting that active α4β1 is required for FXIII-A binding to the plasma membrane (Figure 5a). Further analysis demonstrated that all three integrin inhibitors suppressed the Lys679Met FXIII-A-dependent increase in collagen synthesis (Figure 5b) and proliferation (Figure 5c). These observations suggest that FXIII-A requires α4 integrin to associate with the membrane and promote fibroproliferative responses.

FXIII-A has previously been suggested to associate with integrins through the isoleucine-leucine-aspartate-threonine (ILDT) amino acid motif located on the catalytic domain (Isobe et al., 1999). To test this hypothesis, site-directed mutagenesis was performed to mutate the ILDT motif to AAAA in FXIII-A and define the potential role of this site in regulating fibro-proliferative phenotypes. We found that the mutation of ILDT to AAAA resulted in the inhibition of the FXIII-A-induced increase in both collagen production and proliferation (Figure 5d and e). These data support the concept that FXIII-A can bind to α4 through the ILDT motif and that this region may cooperate with the residues around Lys679 to promote α4 association.

### FXIII-A regulates mitogen-activated protein kinase and phosphatidylinositol 3 kinase activation

To further investigate the potential mechanisms by which FXIII-A promotes cell proliferation and collagen synthesis, we analyzed the activation of a range of different signaling pathways in cells treated with the WT or Lys679Met FXIII-A. Tissue transglutaminase has been reported to promote platelet-derived growth factor receptor-integrin association, and we therefore hypothesized that FXIII-A binding may enhance the activation of this pathway (Zemskov et al., 2009). Western blotting analysis of the cells treated with WT or Lys679Met FXIII-A revealed no significant increase in platelet-derived growth factor receptor activity (as judged by pTyr-751 reactivity, Figure 6a). There were also no detectable changes in the activity of the small guanosine triphosphatase RhoA, that is known to be activated downstream of the integrins and can contribute to collagen synthesis (Supplementary Figure S3e). However, further analysis of other downstream signaling targets (Akt, extracellular signal–regulated kinase1/2, p38alpha) revealed that p-Akt and phospho-extracellular signal–regulated kinase both showed significantly increased activation levels in cells following 1 hour of treatment with both WT and Lys679Met FXIII-A (Figure 6a–c). Taken together, these data suggest that FXIII-A can promote activation of Akt and mitogen-activated protein kinase pathways, which may potentially increase cell proliferation (Figure 6d).

## DISCUSSION

Dermatofibroma is a common benign fibro-histiocytic skin tumor, but little is known about its pathogenesis (Hsi and Nickoloff, 1996). Typically, dermatofibromas are thought to be induced by trauma, particularly following insect bites. Here, we investigated two unrelated pedigrees with autosomal dominant familial multiple dermatofibromas and identified a heterozygous missense mutation in FXIII-A. On one level, this is a surprising finding given that FXIII-A antibodies have been used for the last 40 years for the immunohistochemical diagnosis of dermatofibromas (Cerio et al., 1988). Nevertheless, we also demonstrated that the mutant FXIII-A protein has a functional impact with reduced cross-linking activity but increased fibroblast cell proliferation and adhesion and type I collagen synthesis. Thus, FXIII-A is not only a useful immunohistochemical marker for dermatofibromas, but it is also directly implicated in the molecular genetics of families with multiple dermatofibromas, at least in this study.

FXIII-A is found mainly in macrophages and other cell types including fibroblast-like mesenchymal cells and is expressed in many fibrovascular tumors (Cerio et al., 1989; Nemeth and Penneys, 1989). Indeed, in dermatofibromas, aside from fibroblasts, the main cellular component comprises cells of monocyte or macrophage lineage, and it is these cells that mainly express FXIII-A. In addition, FXIII-A is also present in platelet granules (Muszbek et al., 2011). Therefore, our working hypothesis is that an insect bite or direct trauma may promote a bleed (hemosiderin is common in dermatofibromas, Figure 1c lower image). This bleeding may be enhanced by the presence of Lys679Met FXIII-A, which shows reducing clot stabilization function (but no clinical bleeding abnormality). The small bleed then triggers

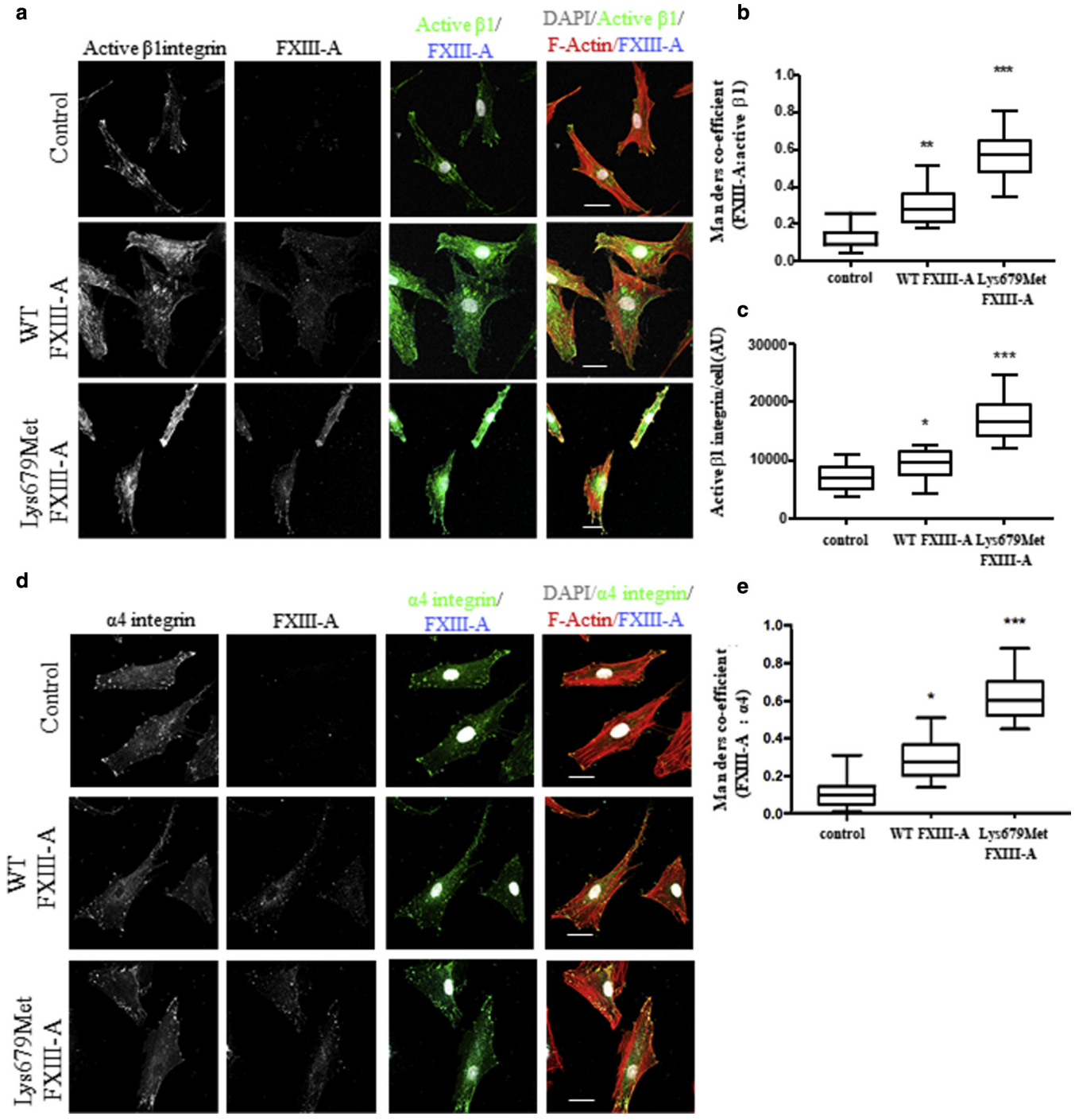


**Figure 4. Co-localization of α4, β1, and FXIII-A on the cell surface suggests that FXIII-A binds to α4β1 integrin.** Immunofluorescence staining and confocal microscopy of fixed, permeabilized NHDFs on coverslips after treatment with WT FXIII-A or Lys679Met FXIII-A for 2 hours before fixation. (**a**) Images show co-localization of active β1integrin and FXIII-A after treatment with either WT or mutant FXIII-A. Bar = 10 um. (**b**) Manders overlap co-efficient analyses showing the percentage overlap between FXIII-A and active β1integrin is greater for Lys679Met FXIII-A. (**c**) Level of Active β1 integrin intensity per cell is greater for Lys679Met FXIII-A. (**d**) Images show the co-localization of α4 integrin and FXIII-A, which is greater for Lys679Met FXIII-A compared with WT FXIII-A. Bar = 10 um. (**e**) Manders overlap co-efficient analysis showing that the percentage overlap between FXIII-A and integrin is greater for Lys679Met FXIII-A. All the experiments were done in triplicate. The data represent the means ± SD for three experiments. *$P < 0.05$ vs control, **$P < 0.01$ vs control. ***$P < 0.001$ vs control. FXIII-A, factor XIII subunit A; NHDFs, normal human dermal fibroblasts; WT, wild type.

platelet plug formation, platelet granule degradation, and the release of FXIII-A that then impacts on fibroblast cell biology and collagen production. Still to be explored and currently unexplained, however, is the role of mutant FXIII-A in monocytes or macrophages.

Previously, autosomal recessive mutations in FXIII-A (mostly A-subunit, rarely B) have been identified in very rare bleeding disorders (incidence ~1 in 5 million), sometimes with wound healing abnormalities (Karimi et al., 2009), but no pathogenic autosomal dominant mutations have been

previously described. The mutation Lys679Met is not a novel variant but is present in the general population with low frequency (risk allele frequency 0.0207%; rs201302247); the allele is more common among Ashkenazi Jews (Genome Aggregation Database). Our expectation is that other individuals with this heterozygous missense mutation may also have multiple dermatofibromas, although this remains to be proven. Regarding sporadic, non-familial dermatofibromas, we did not find any evidence for *F13A1* genetic variants, and therefore, the role that FXIII-A may play (or not) in such lesions awaits further study.

Previous reports have suggested that recessive mutations within the β-barrel 1 and β- barrel 2 domains of FXIII-A can affect the regions of the protein that regulate conformational changes during activation (Thomas et al., 2016). Our analysis suggests that the Lys679Met mutation is more likely to have an impact on the activation step rather than a direct effect on the catalytic machinery. The exact molecular details of how this might occur are not yet clear.

Two key phenotypes of dermatofibroma are fibroblast proliferation and collagen production. In contrast to reduced coagulation function, the mutation Lys679Met clearly enhances both pro-fibrotic and proliferative effects, as evidenced by the proliferation data and type I collagen quantitative reverse transcriptase in real time, western blots, and CDM production. Our data also suggest that FXIII-A associates with α4β1integrins at the plasma membrane to elicit these phenotypic effects and that this is mediated via the ILDT motif in FXIII-A. Lys679Met FXIII-A may bind with a higher affinity or for a greater length of time to α4 integrins. However, biochemical in vitro studies to assess the direct binding would be required to validate this hypothesis.

We further explored the link between α4 integrin activation and proliferation and collagen synthesis. Published evidence suggests that upon activation, integrins can activate platelet-derived growth factor receptor or LRP-6 (Muramatsu et al., 2004; Ren et al., 2013; Zemskov et al., 2009), although we did not observe any activation in these receptors. We also did not observe changes to the activity of RhoA upon FXIII-A addition to the fibroblasts. We demonstrated significant increases in phospho-extracellular signal–regulated kinase1/2 and p-Akt upon FXIII-A binding, which are key downstream targets in the RAS, RAF, MAPK/ERK pathway, ERK and the phosphatidylinositol 3 kinase/Akt signaling pathways, but there were no differences between the WT and Lys679Met (De Luca et al., 2012). For now, we conclude that the proposed enhanced action of Lys679Met FXIII-A on α4 integrin could initiate different signaling cascades, which remain to be determined (Figure 6d).

In summary, our study provides insight into the genetic and cellular basis of a subset of familial dermatofibromas and highlights an extended role for FXIII-A in their pathobiology.

## MATERIALS AND METHODS

### Whole Exome Sequencing and Sanger Sequencing

Following written informed consent from the patients and institutional ethics committee approval, whole exome sequencing was performed using DNA from available probands and their family members by the Illumina Hi-Seq2500 system (Illumina, San Diego, CA). The Exome capture kit (Agilent SureSelect Human All Exon 50 Mb kit, Santa Clara, CA) was used to prepare DNA libraries from 3 μg of DNA. First, the Adapted Focused Acoustic technology (Covaris, Woburn, MA) was used to shear the genomic DNA to yield a mean of 150 base pair fragment size. The fragment ends were then repaired, ligated with sequencing adaptors, and hybridized against biotinylated 120 base pair RNA probes (Agilent) targeting protein-coding genomic regions for 24 hours. Targeted regions were selected for with magnetic streptavidin-coated beads, while unbound DNA was washed off. The exome-enriched DNA pool was next eluted, amplified with low-cycle PCR, multiplexed (four samples on each lane), and sequenced with 100 base paired-end reads. Reads were aligned to the GRCh37/hg19 reference genome using Novoalign (Novocraft Technologies, Selangor, Malaysia). The Bedtools package and custom scripts were used to calculate the depth of sequence coverage (Quinlan and Hall, 2010). The SAMtools software was used for variant calling and quality filtering (Li et al., 2009). Variants were then annotated with multiple passes through the ANNOVAR software package (Wang et al., 2010). PCR and Sanger sequencing were performed to validate the segregation of the mutation with phenotypes according to standard protocol using primers for *F13A1* exon14 (Supplementary Table S5).

### Purification of FXIII-A- glutathione S-transferase fusion proteins for functional analysis

pGEX-FXIII-A, an expression vector encoding an N-terminal glutathione S-transferase-FXIII-A fusion protein, was generated as previously described (Smith et al., 2011). The Lys679Met FXIII-A variant was generated by site-directed mutagenesis using the primers listed (Supplementary Table S7) with a QuickChange II Kit (Agilent Technologies; Stockport, United Kingdom). Successful mutagenesis was verified by DNA sequencing. Both FXIII-A plasmids were then transformed into XL10-Gold Ultra-competent *E. coli* (Agilent Technologies, Wokingham, United Kingdom). FXIII-$A_2$ Expression and purification were performed as previously described (Duval et al., 2016).

### FXIII-A activity analysis by Pentylamine Incorporation

The FXIII activity was measured using a modified 5-(biotinamido) pentylamine incorporation assay. Nunc-Immuno 96 Micro-Well plates were coated with 100 μl of 10 μg/ml N, N-dimethylated casein overnight at 4 °C, then blocked with 300 μl 1% BSA in Tris buffer saline (TBS) for 90 minutes at 37 °C. The plates were then washed with 4x 300 μl TBS and 10 μl of samples (WT or Lys679Met rhFXIII-$A_2$ or murine plasma) were added to the wells in triplicate. To the wells, 90μl of activation mix (111 μM dithiothreitol, 0.3 μM biotinylated pentylamine, 11 mM $CaCl_2$, and 2.2 U/ml thrombin) was added, and the reactions were stopped at 0, 20, 40, 60, 80, 100, and 120 minutes by adding 200 μl of 200 mM EDTA. The plates were washed with 4x 300 μl 0.1% (v/v) Tween 20 in TBS, and 100 μl of 2 μg/ml of streptavidin in 1% (w/v) BSA (in TBS-Tween) was added for 60 minutes at 37 °C. Following washes with 4x 300 μl TBS-Tween, 100 μl of 1 mg/ml phosphatase substrate (in 1 M diethanolamine) was added, and the reaction was stopped by adding 100 μl of 4 M NaOH. The absorbance was measured at 405 nm using a SpectraMax 190 absorbance microtiter plate reader (Molecular Devices, Wokingham, United Kingdom). The rate of pentylamine incorporation over time was then used as an indicator of PreScission-cleaved FXIII activity. The experiments were performed in triplicate.

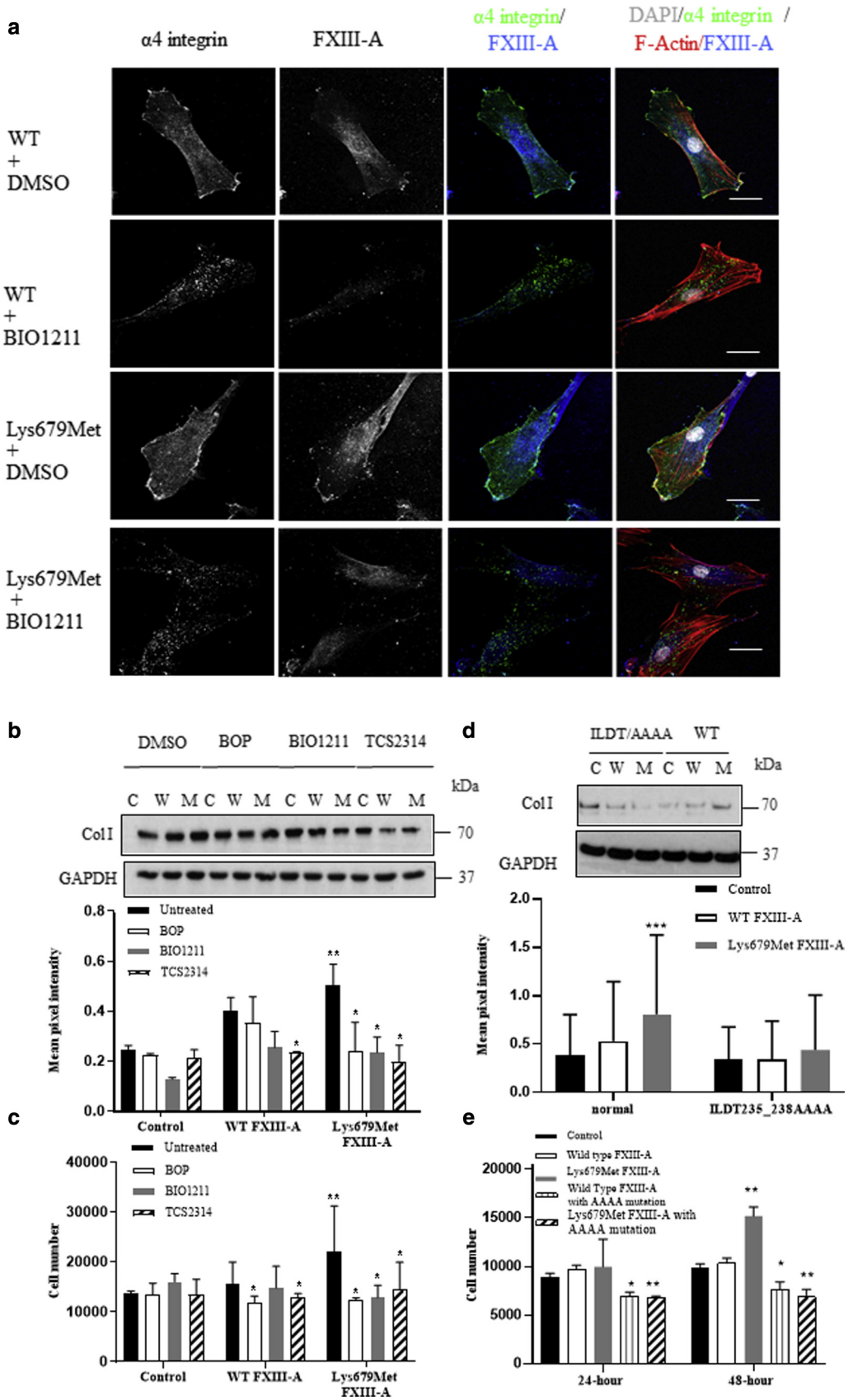


**Figure 5. FXIII-A associates with α4β1integrin via the ILDT motif in FXIII-A.** (**a**) NHDFs on the coverslips were pre-treated with either DMSO (control) or BIO1211 (α4β1 integrin inhibitor) for 2 hours and then WT FXIII-A, Lys679Met FXIII-A and control conditioned media was added for 1 hour. Confocal images show that BIO1211 induces the internalization of α4 integrin (small green dots); there is less FXIII-A binding for both the WT and Lys679Met FXIII-A when the cells are incubated with BIO1211. Bar = 10 um. (**b**) Western blots show reduction in collagen I expression after incubation with three different integrin

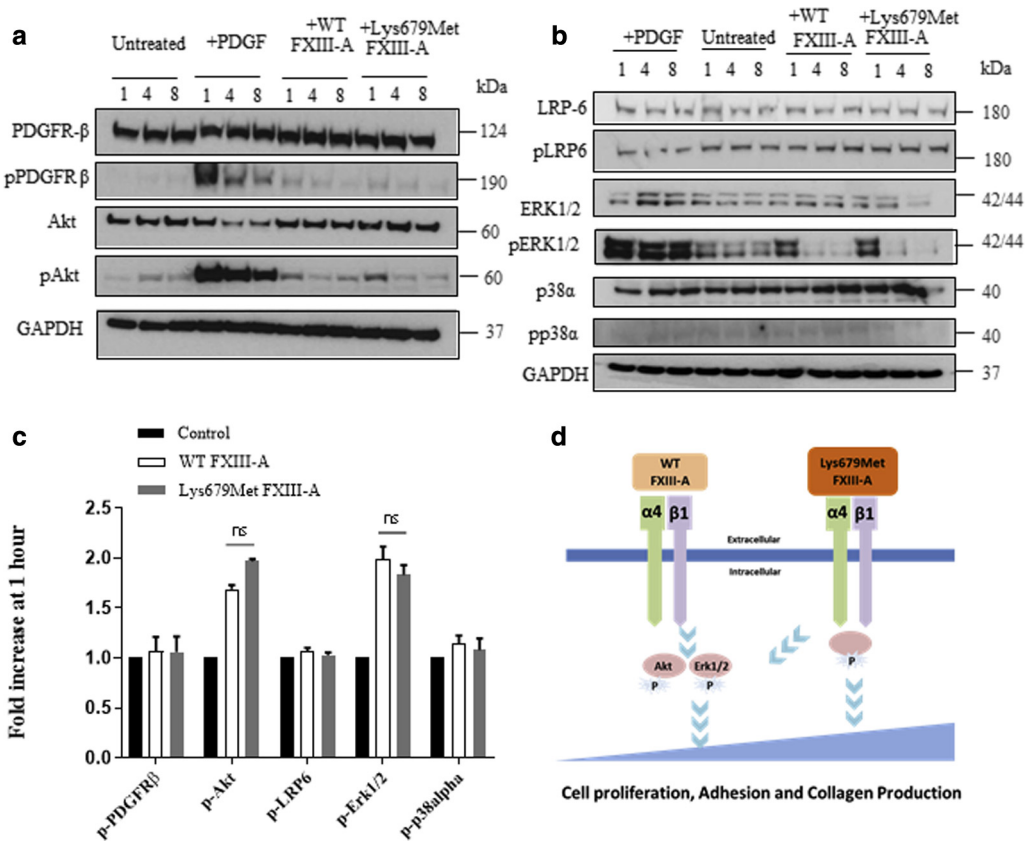


**Figure 6. WT and Lys679Met FXIII-A both increase Akt and ERK1/2 activation.** (**a**) NHDFs were treated with FXIII-A for 1, 4, or 8 hours with a 2 nM PDGF-BB treatment as a positive control. The activation levels of PDGFR and Akt were determined by immunoblotting with antibodies to Tyr (p)-751-PDGFRβ and Ser(p)-473-Akt1. All the samples were normalized for equal amounts with GAPDH. No activation was noted for p-PDGFR, whereas both WT and Lys679Met FXIII-A showed a transient increase in p-Akt signaling at 1 hour. (**b**) Activation level of LRP-6, ERK1/2, and p38α were determined by immunoblotting with antibodies to Ser (p)-1490-LRP6, Thr202 (p)/Thr204 (p)-p44/42MAPK (ERK1/2), and Thr (p)-180)/Tyr (p)-182-p38α. All the samples were normalized for equal amounts with GAPDH. Both WT and Lys679Met FXIII-A showed transient increase in p-ERK1/2 signaling at 1 hour. (**c**) Phosphoproteins were quantified, averaged, and expressed for NHDF cells treated with WT and Lys679Met FXIII-A as a fold change over those of the untreated cells. Both WT and Lys679Met FXIII-A showed similar ~two-fold increases in p-Akt and p-ERK1/2 compared to the control. Shown are the means ± SD for three experiments. (**d**) A proposed schematic figure for FXIII-A and α4β1 integrin association on the cell surface and downstream signaling. Lys679Met may lead to a conformational change in the protein, which promotes α4 integrin binding (right panel). WT and Lys679Met FXIII-A after association with the integrins activate Akt and ERK1/2, resulting in cell proliferation, adhesion, and collagen production. However, the enhanced action of mutant FXIII-A on α4 integrin could initiate different signaling cascades, which still remain to be determined. Akt, protein kinase B; ERK, extracellular signal–regulated kinase; FXIII-A, factor XIII subunit A; GADPH, glyceraldehyde-3-phosphate dehydrogenase; NHDFs, normal human dermal fibroblasts; PDGFR, platelet-derived growth factor receptor; WT, wild type.

### Normal human dermal fibroblast and HEK293 cell culture

Normal human dermal fibroblasts (Cellworks, Buckingham, United Kingdom) up to passage number 10 and HEK293 cells (ATCC; Middlesex, United Kingdom) were cultured in DMEM in high glucose (4.5g/l), 10% (v/v) fetal bovine serum, 50 μg/ml penicillin, and 2 mM L-glutamine in a humidified incubator at 37 °C with 5% $CO_2$. Cells were tested for Mycoplasma infection with the Mycoalert Mycoplasma Detection Kit (Lonza, Slough, United Kingdom).

### Plasmid constructs, site-directed mutagenesis, and FXIII-A expression in the HEK293 cell line

Site-directed mutagenesis was performed on the mammalian expression vector pIRES2-EGFP containing the cDNA FXIII-A (a kind gift from Jayo et al., 2009) according to the QuikChange Lightning Site-Directed Mutagenesis Kit protocol (Agilent Technologies) using primers (Supplementary Table S7). Transient transfection was performed using Lipofectamine 3000 on the HEK293 cell line. Transfected cells were grown in media containing 2% fetal bovine serum for 48 hours before collecting the conditioned media for experiments. The FXIII-A expression level was verified by western blotting.

### Proliferation, adhesion assays, and cell-derived matrix (CDM) preparation

Fibroblasts were plated in media containing 2% serum 1 day before the experiment. The cells were then treated with conditioned media containing either WT or Lys679Met FXIII-A for 24 and 48 hours for

inhibitors (BIO1211, BOP, TCS2314), particularly for cells treated with Lys679Met FXIII-A compared to WT FXIII-A. (**c**) Graph shows reduced cell proliferation rates following FXIII-A treatment (WT or Lys679Met) compared to control after incubation with the three integrin inhibitors at 48 hours. (**d**) Western blot shows the reduction of Collagen I expression after 48-hour treatment with ILDT235_238AAAA FXIII-A. (**e**) Graph shows the reduced cell proliferation rate after the site-directed mutagenesis of ILDT motif of FXIII-A. These effects for (f) and (g) are common to the WT and Lys679Met FXIII-A but are more marked with Lys679Met FXIII-A. Experiments were performed in triplicate. The data show means ± SD for three experiments. *$P < 0.05$ vs control **$P < 0.01$ vs control ***$P < 0.001$ vs control. C, control; FXIII-A, factor XIII subunit A; M, mutant; NHDFs, normal human dermal fibroblasts; WT, wild type.

the proliferation assay. Collagen type I solution from rat tail (Sigma-Aldrich, St. Louis, MO) at a concentration of 50 μg/ml was used to coat a plate for adhesion assays. For CDM preparation, the cells were grown on 0.2% crosslinked gelatin-coated coverslips for 14 days before cell denudation as previously described (Kaukonen et al., 2017). The cells and matrices were then fixed for 10 minutes at room temperature with a 4% final concentration of paraformaldehyde. The cells were permeabilized with 0.1% Triton-X100 in phosphate buffered saline solution for 10 minutes followed by a 1-hour incubation with 3% BSA in phosphate buffered saline solution containing 1:400 phalloidin-AlexaFluor488 and 1:1,000 DAPI. The images of cells were acquired by tile-scans of each well using EVOSTM FL Auto 2 Imaging System (ThermoFisher, Waltham, MA) with a ×10 objective lens. The number of cells in each well was measured by automated nuclei counting using ImageJ software (NIH, Bethesda, MD).

### Reverse Transcription PCR

Fibroblasts were treated with WT and Lys679Met FXIII-A for 48 hours. Total RNA was extracted using an RNeasy Micro Kit (Qiagen, Venlo, The Netherlands). The quality of RNA was analyzed by a Nanodrop spectrophotometer (ThermoFisher). Reverse transcription was performed using a High-Capacity cDNA Reverse Transcription Kit according to the manufacturer's instructions. Gene expression was assessed by real-time PCR by using TagMan Gene Expression Assays for *Col1a1* Mm00801666_g1 (ThermoFisher). Transcript levels were normalized to glyceraldehyde-3-phosphate dehydrogenase expression and measured with Applied Biosystems (Foster City, CA) TaqMan probes.

### Western blot analysis

Whole cell lysates of fibroblasts were collected after treatment with FXIII-A conditioned media using radioimmunoprecipitation buffer with protease inhibitor cocktail set I (Calbiochem, San Diego, CA). Each sample was resuspended in NuPAGE LDS Sample Buffer (Invitrogen), boiled at 100 °C for 5 minutes, and run on NuPAGE 4-12% Bis-Tris Protein Gels (Invitrogen). The resolved proteins were transferred and blotted onto a nitrocellulose membrane. Primary and secondary antibodies are listed (Supplementary Table S8).

### Immunofluorescence and confocal microscopy

Fibroblasts on the coverslips were treated with WT and Lys679Met FXIII-A over variable time points, then washed and fixed with 4% paraformaldehyde in phosphate buffered saline before 10-minute permeabilization with 0.1% Triton-X100, followed by blocking with 5% BSA in phosphate buffered saline for 30 minutes. The cells were labeled with antibodies (Supplementary Table S8) at 4 °C overnight and then stained with secondary antibodies (Supplementary Table S8), phalloidin-AlexaFluor568, and DAPI. The cells were imaged with a ×60 objective using Nikon A1R inverted confocal microscope (Nikon, Amsterdam, The Netherlands). Images were exported from the Nikon Elements software for further analysis in ImageJ software using intensity functions of the co-localization analysis plugin JaCoP.

### Data Availability Statement

Datasets related to this article can be found at https://www.ncbi.nlm.nih.gov/bioproject/ PRJNA545215, hosted at Sequence Read Archive (SRA) under the collection ID PRJNA545215.

### ORCIDs

Chavalit Supsrisunjai: https://orcid.org/0000-0002-1054-6918
Chao-Kai Hsu: https://orcid.org/0000-0003-4365-4533
Magdalene Michael: https://orcid.org/0000-0003-2577-729X
Cédric Duval: https://orcid.org/0000-0002-4870-6542
John Y. W. Lee: https://orcid.org/0000-0002-5563-2334
Hsing-San Yang: https://orcid.org/0000-0002-3973-2896
Hsin-Yu Huang: https://orcid.org/0000-0003-0220-3509
Thitiwat Chaikul: https://orcid.org/0000-0001-5463-3864
Alexandros Onoufriadis: https://orcid.org/0000-0001-5026-0431
Roberto Steiner: https://orcid.org/0000-0001-7084-9745
Robert A. S. Ariëns: https://orcid.org/0000-0002-6310-5745
Ofer Sarig: https://orcid.org/0000-0003-2987-2091
Eli Sprecher: https://orcid.org/0000-0003-0666-0045
Marina Eskin-Schwartz: https://orcid.org/0000-0003-0507-1505
Curt Samlaska: https://orcid.org/0000-0001-7562-4254
Michael A. Simpson: https://orcid.org/0000-0002-8539-8753
Eduardo Calonje : https://orcid.org/0000-0001-7475-6423
Maddy Parsons: https://orcid.org/0000-0002-2021-8379
John A. McGrath: https://orcid.org/0000-0002-3708-9964

### CONFLICT OF INTEREST

The authors state no conflicts of interest.

### ACKNOWLEDGMENTS

The authors acknowledge financial support from the Rosetrees Trust, Medical Research Council UK (MR/M018512/1) and the National Institute for Health Research (NIHR) Biomedical Research Centre based at Guy's and St Thomas' NHS Foundation Trust, King's College London, U.K and Department of Medical Services, Ministry of Public Health, Thailand.

MP and JAM are joint senior authors for this study.

### AUTHOR CONTRIBUTIONS

Conceptualization: CS, MP, JAM; Investigation: CS, CKH, MM, CD, JYWL, TC, RS, RASA, MP; Formal Analysis: CS CKH, CD, TC, AO, MAS, JEC, MP; Methodology: CS, CKH, MP; Resources: H-SY, H-Y H, OS, ES, MS-E, CuS; Supervision: MP, JAM; Writing — original draft: CS; Writing — review & editing: CS, MP, and JAM

### SUPPLEMENTARY MATERIAL

Supplementary material is linked to the online version of the paper at www.jidonline.org, and at https://doi.org/10.1016/j.jid.2019.08.441.

### REFERENCES

Altman DA, Nickoloff BJ, Fivenson DP. Differential expression of factor XIIIa and CD34 in cutaneous mesenchymal tumors. J Cutan Pathol 1993;20:154–8.

Bagoly Z, Katona E, Muszbek L. Factor XIII and inflammatory cells. Thromb Res 2012;129(Suppl. 2):S77–81.

Beatrous SV, Riahi RR, Grisoli SB, Cohen PR. Associated conditions in patients with multiple dermatofibromas: case reports and literature review. Dermatol Online J 2017;23.

Cerio R, Griffiths CE, Cooper KD, Nickoloff BJ, Headington JT. Characterization of factor XIIIa positive dermal dendritic cells in normal and inflamed skin. Br J Dermatol 1989;121:421–31.

Cerio R, Spaull J, Jones EW. Identification of factor XIIIa in cutaneous tissue. Histopathology 1988;13:362–4.

De Luca A, Maiello MR, D'Alessio A, Pergameno M, Normanno N. The RAS/RAF/MEK/ERK and the PI3K/AKT signalling pathways: role in cancer pathogenesis and implications for therapeutic approaches. Expert Opin Ther Targets 2012;16(Suppl. 2):S17–27.

Duval C, Ali M, Chaudhry WW, Ridger VC, Ariëns RA, Philippou H. Factor XIII A-subunit V34L variant affects Thrombus cross-linking in a murine model of thrombosis. Arterioscler Thromb Vasc Biol 2016;36:308–16.

Hsi ED, Nickoloff BJ. Dermatofibroma and dermatofibrosarcoma protuberans: an immunohistochemical study reveals distinctive antigenic profiles. J Dermatol Sci 1996;11:1–9.

Isobe T, Takahashi H, Ueki S, Takagi J, Saito Y. Activity-independent cell adhesion to tissue-type transglutaminase is mediated by alpha4beta1 integrin. Eur J Cell Biol 1999;78:876–83.

Jakobiec FA, Rai R, Yoon MK. Fibrous histiocytoma of the tarsus: clinical and immunohistochemical observations with a differential diagnosis. Cornea 2014;33:536–9.

Jakobiec FA, Zakka FR, Tu Y, Freitag SK. Dermatofibroma of the eyelid: immunohistochemical diagnosis. Ophthal Plast Reconstr Surg 2017;33:e134–8.

Jayo A, Conde I, Lastres P, Jiménez-Yuste V, González-Manchón C. Possible role for cellular FXIII in monocyte-derived dendritic cell motility. Eur J Cell Biol 2009;88:423–31.

Karimi M, Bereczky Z, Cohan N, Muszbek L. Factor XIII deficiency. Semin Thromb Hemost 2009;35:426–38.

Kaukonen R, Jacquemet G, Hamidi H, Ivaska J. Cell-derived matrices for studying cell proliferation and directional migration in a complex 3D microenvironment. Nat Protoc 2017;12:2376–90.

Kluger N, Cotten H, Magana C, Pinquier L. Dermatofibroma occurring within a tattoo: report of two cases. J Cutan Pathol 2008;35:696–8.

Komáromi I, Bagoly Z, Muszbek L. Factor XIII: novel structural and functional aspects. J Thromb Haemost 2011;9:9–20.

Li H, Handsaker B, Wysoker A, Fennell T, Ruan J, Homer N, et al. The Sequence Alignment/Map format and SAMtools. Bioinformatics 2009;25:2078–9.

Muramatsu H, Zou P, Suzuki H, Oda Y, Chen GY, Sakaguchi N, et al. alpha4beta1- and alpha6beta1-integrins are functional receptors for midkine, a heparin-binding growth factor. J Cell Sci 2004;117:5405–15.

Muszbek L, Bereczky Z, Bagoly Z, Komáromi I, Katona É. Factor XIII: a coagulation factor with multiple plasmatic and cellular functions. Physiol Rev 2011;91:931–72.

Myers DJ, Fillman EP. Dermatofibroma. In: StatPearls [Internet]. Treasure Island (FL): StatPearls Publishing; 2019.

Nemeth AJ, Penneys NS. Factor XIIIa is expressed by fibroblasts in fibrovascular tumors. J Cutan Pathol 1989;16:266–71.

Quinlan AR, Hall IM. BEDTools: a flexible suite of utilities for comparing genomic features. Bioinformatics 2010;26:841–2.

Ren S, Johnson BG, Kida Y, Ip C, Davidson KC, Lin SL, et al. LRP-6 is a coreceptor for multiple fibrogenic signaling pathways in pericytes and myofibroblasts that are inhibited by DKK-1. Proc Natl Acad Sci USA 2013;110:1440–5.

Samlaska C, Bennion S. Eruptive dermatofibromas in a kindred. Cutis 2002;69:187–8. 190.

Smith KA, Adamson PJ, Pease RJ, Brown JM, Balmforth AJ, Cordell PA, et al. Interactions between factor XIII and the alphaC region of fibrinogen. Blood 2011;117:3460–8.

Stieler M, Weber J, Hils M, Kolb P, Heine A, Büchold C, et al. Structure of active coagulation factor XIII triggered by calcium binding: basis for the design of next-generation anticoagulants. Angew Chem Int Ed Engl 2013;52:11930–4.

Thomas A, Biswas A, Dodt J, Philippou H, Hethershaw E, Ensikat HJ, et al. Coagulation factor XIIIA subunit missense mutations affect structure and function at the various steps of factor XIII action. Hum Mutat 2016;37:1030–41.

Wang K, Li M, Hakonarson HH. ANNOVAR: Functional annotation of genetic variants from high-throughput sequencing data. Nucleic Acids Res 2010;38:e164.

Weiss MS, Metzner HJ, Hilgenfeld R. Two non-proline cis peptide bonds may be important for factor XIII function. FEBS Lett 1998;423:291–6.

Yee VC, Pedersen LC, Le Trong I. Bishop PD, Stenkamp RE, Teller DC. Three-dimensional structure of a transglutaminase: human blood coagulation factor XIII. Proc Natl Acad Sci USA 1994;91:7296–300.

Zelger BG, Zelger B. Dermatofibroma: a clinico-pathologic classification scheme. Pathologe 1998;19:412–9.

Zemskov EA, Loukinova E, Mikhailenko I, Coleman RA, Strickland DK, Belkin AM. Regulation of platelet-derived growth factor receptor function by integrin-associated cell surface transglutaminase. J Biol Chem 2009;284:16693–703.

## SUPPLEMENTARY MATERIALS AND METHODS AND RESULTS

We performed Sanger sequencing on 22 Taiwanese sporadic dermatofibroma samples and 28 in-house sporadic dermatofibromas samples to determine whether Lys679Met variants and other potential variants are present in any sporadic dermatofibromas. We also hypothesized that variants in the promoter region of *F13A1* might be associated with sporadic dermatofibroma. In order to determine single nucleotide polymorphisms (SNPs) in this area, Sanger sequencing was performed on the *F13A1* gene and its promoter region. Regarding promoter region sequencing, we divided the promoter region (2400 bases) into five segments that overlapped each other. The length of each segment was approximately 500 bases. Forward and reverse primers for each segment were designed by using an online tool (Primer 3) resulted in five pairs of primers (Supplementary Table S6). A total of 50 sporadic dermatofibroma were sequenced for the *F13A1* gene and 22 DNA samples for the promoter region. AmpliTaq Gold 360 Master Mix (ThermoFisher) and the PCR protocol were used as previously described. The ABI 3730 DNA Sequencher (SeqGen, CA) was then used to analyze the sequence. The allele frequencies of each SNP were compared with population databases, that is, the 1000 Genome Project and Exome Aggregation Consortium Browser, where available. For unreported SNPs, we compared with 30 in-house Taiwanese control samples. All 50 sporadic dermatofibroma were successfully sequenced for an additional SNP analysis. The total of three variants in *F13A1* and five variants in the promoter region were identified from Sanger sequencing (Supplementary Tables S3 and S4). None of these variants was statistically significant and different from the variants in the population database as compared by using the Hardy-Weinberg equilibrium calculation and chi-square test (GraphPad Prism version 8, San Diego, CA).

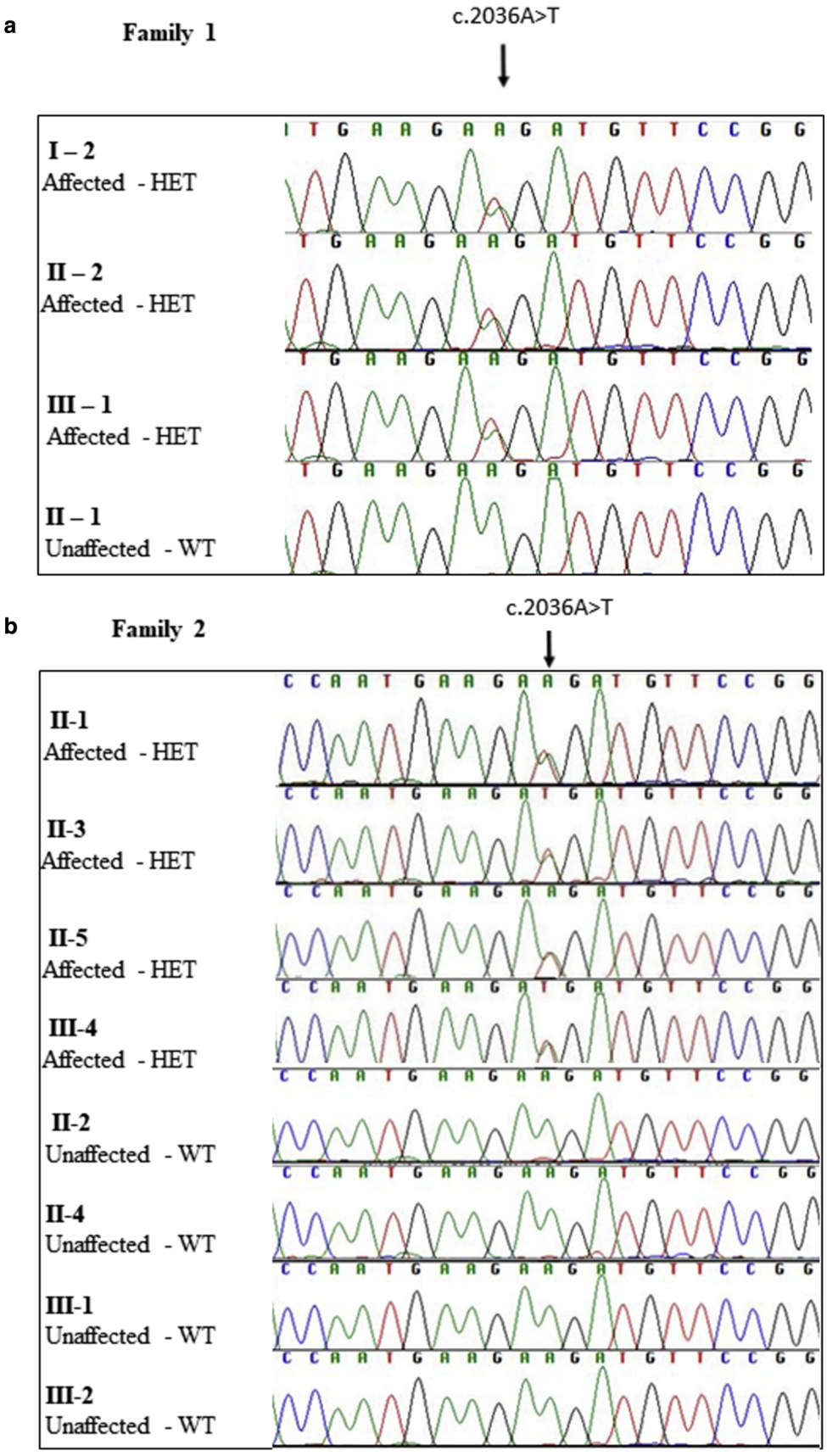


**Supplementary Figure 1.**
Chromatograms of *F13A1* gene reveals the heterozygous variant c.2036A>T (Lys679Met) in all affected subjects.

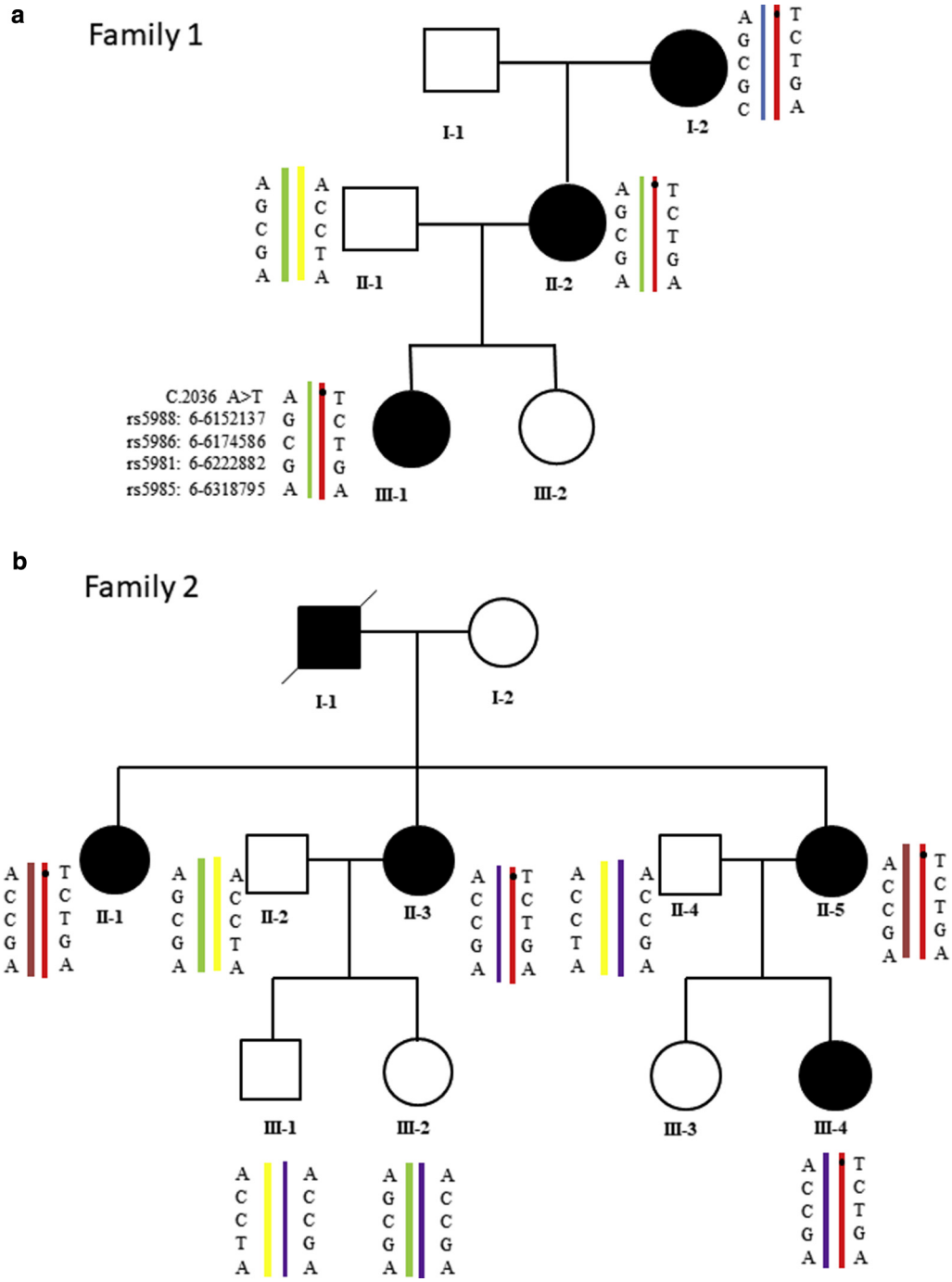


**Supplementary Figure 2. Haplotype analysis supports a common ancestral *F13A1* mutant allele in families 1 and 2.** (**a, b**) SNP genotyping of two individuals in two families and their relatives with four highly polymorphic markers within *F13A1* shows that the individuals share the same haplogroup for the *F13A1* containing c.2036A>T (indicated by black spot). Each color bar represents a distinct haplotype.

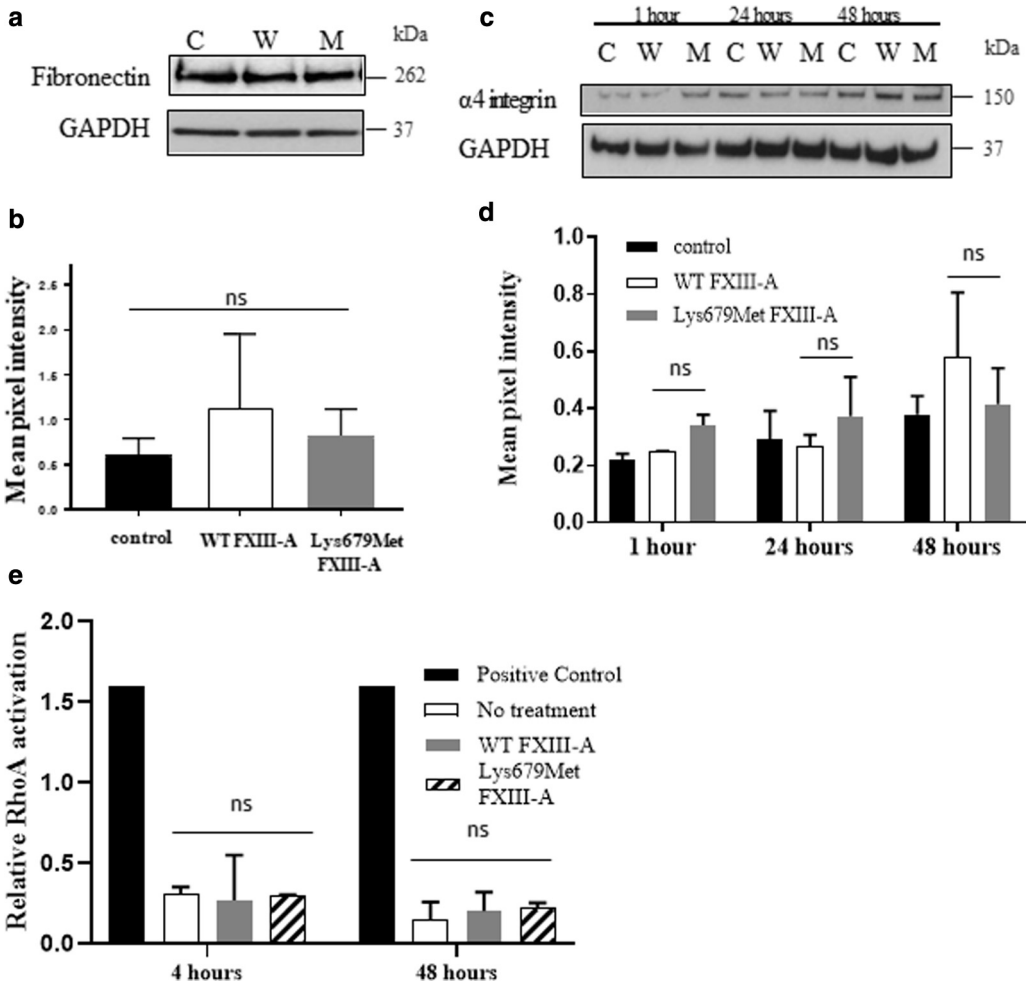


**Supplementary Figure 3. Levels of fibronectin and α4 integrin show no significant differences between treatments with either wild-type or mutant FXIII.** (**a, b**) NHDFs were treated with FXIII-A for 48 hours with WT and Lys679Met FXIII-A; level of fibronectin was determined by immunoblotting with antibodies to fibronectin. (**c, d**) NHDFs were treated with FXIII-A for 1, 24, 48 hours with WT and Lys679Met FXIII-A; level of α4 integrin was determined by immunoblotting. All samples were normalized for equal amounts with GAPDH. (**e**) NHDFs were treated with FXIII-A for 4 and 48 hours; level of RhoA was determined by GTPase- enzyme linked immunoabsorbent assay (G-LISA) Activation assays protocol (Cytoskeleton, Denver, CO). Data are shown as mean ± SD for three experiments.

## Supplementary Table S1. A Summary of the Stepwise Filtering Approach to Identify a Potentially Shared Variant

| | Family 1 (Ukraine) | | | Family 2 (USA) | | | | |
|---|---|---|---|---|---|---|---|---|
| **Pedigrees** | **I-2** | **II-2** | **III-1** | **II-1** | **II-3** | **II-2** | **III-2** | **II-5** |
| Total variants | 26,063 | 26,327 | 26,278 | 26,006 | 26,072 | 26,061 | 26,236 | 25,818 |
| Variants with MAF < 0.01 in 1,000 genomes, ESP, ExAC, and 6,000 control exomes | 1,098 | 870 | 849 | 911 | 893 | 952 | 936 | 881 |
| Heterozygous variants | 768 | 850 | 833 | 872 | 866 | 918 | 910 | 852 |
| Heterozygous nonsynonymous, splice-site, or insertion/deletion variants | 556 | 541 | 526 | 530 | 496 | 578 | 808 | 530 |
| Shared variants among affected individuals | | 118 | | | | 113 | | |
| Genes with variants that are shared between the two pedigrees | | | | | 1 (*F13A1*) | | | |

Abbreviations: ESP, NHLBI Exome Sequencing Project; EXAC, Exome Aggregation Consortium; MAF, minor allele frequency.

## Supplementary Table S2. A Summary of the Statistics of Exome Sequencing and Coverage

| | USA family | | | | | Ukraine family | | |
|---|---|---|---|---|---|---|---|---|
| **Case** | **II-1** | **II-3** | **II-2** | **III-2** | **II-5** | **I-2** | **II-2** | **III-1** |
| Total reads | 75,853,390 | 80,748,322 | 55,446,430 | 86,094,748 | 68,319,976 | 92,053,964 | 103,018,007 | 106,717,428 |
| Reads uniquely mapped to ± 150 bp of the target sequence | 41,705,779 (54.98%) | 43,183,922 (53.48%) | 30,637,737 (55.26%) | 47,083,150 (54.69%) | 35,757,820 (52.34%) | 71,957,989 (78.17%) | 80,224,711 (77.87%) | 83,043,872 (77.82%) |
| Reads uniquely mapped to target sequence | 38,934,653 (51.33%) | 40,209,995 (49.8%) | 28,501,204 (51.4%) | 43,584,762 (50.62%) | 33,379,406 (48.86%) | 65,046,797 (70.66%) | 72,451,957 (70.33%) | 74,728,981 (70.03%) |
| Mean_ Coverage (reads per position) | 81.49 | 82.54 | 58.58 | 90.98 | 67.89 | 122.86 | 136.85 | 140.54 |
| Target CCDS bases | 33,323,618 | 33,323,618 | 33,323,618 | 33,323,618 | 33,323,618 | 33,323,618 | 33,323,618 | 33,323,618 |
| CCDS bases with coverage > 1x | 33,113,976 (99.37%) | 33,109,377 (99.36%) | 33,140,600 (99.45%) | 33,147,115 (99.47%) | 33,067,174 (99.23%) | 32,979,225 (98.97%) | 33,001,727 (99.03%) | 33,003,929 (99.04%) |
| CCDS bases with coverage > 5x | 32,754,189 (98.29%) | 32,721,647 (98.19%) | 32,734,490 (98.23%) | 32,792,592 (98.41%) | 32,528,456 (97.61%) | 32,753,490 (98.29%) | 32,795,207 (98.41%) | 32,789,252 (98.4%) |
| CCDS bases with coverage > 10x | 32,241,535 (96.75%) | 32,181,220 (96.57%) | 31,910,596 (95.76%) | 32,289,315 (96.9%) | 31,807,387 (95.45%) | 32,513,166 (97.57%) | 32,600,284 (97.83%) | 32,581,726 (97.77%) |
| CCDS bases with coverage > 20x | 31,106,314 (93.35%) | 31,018,109 (93.08%) | 29,043,630 (87.16%) | 31,234,256 (93.73%) | 30,095,747 (90.31%) | 31,826,135 (95.51%) | 32,059,438 (96.21%) | 32,031,001 (96.12%) |

Abbreviations: bp, base pair; CCDS, Consensus coding sequence.

## Supplementary Table S3. Hardy-Weinberg Equilibrium and Chi-Square test for Analysis of SNPs in *F13A1* from Sporadic Dermatofibromas

| | Homozygous variant | | Heterozygous variant | | Wild type | | |
|---|---|---|---|---|---|---|---|
| **Variant** | **Observed #** | **Expected #** | **Observed #** | **Expected #** | **Observed #** | **Expected #** | ***P-value* (two- tailed)** |
| rs5982 (c.1694C>T) | 3 | 4.67 | 18 | 21.09 | 27 | 22.24 | 0.3561 |
| rs5987 (c.1951G>A) | 0 | 0.4 | 6 | 8.62 | 42 | 38.98 | 0.4889 |
| rs5988 (c.1954G>C) | 0 | 0.41 | 7 | 8.69 | 41 | 38.89 | 0.6517 |

## Supplementary Table S4. Hardy-Weinberg Equilibrium and Chi-Square Test for Analysis of SNPs in *F13A1* Promoter Region from Sporadic Dermatofibromas

| | Homozygous variant | | Heterozygote | | Homozygous reference | | |
|---|---|---|---|---|---|---|---|
| Variant | Observed # | Expected # | Observed # | Expected # | Observed # | Expected # | *P*-value (two- tailed) |
| rs1024231 | 9 | 8.715 | 9 | 9.996 | 3 | 2.289 | 0.8481 |
| rs2815822 | 21 | 18.84 | 0 | 2.121 | 0 | 0.042 | 0.2995 |
| rs1016925 | 0 | 0.42 | 5 | 6.867 | 13.71 | 16 | 0.5197 |
| rs1267856 | 0 | 2.06 | 8 | 8.84 | 12 | 9.1 | 0.2161 |
| rs1267855 | 2 | 2.74 | 7 | 9.44 | 11 | 7.82 | 0.3458 |

## Supplementary Table S5. Primers for *F13A1*

| Exon | Forward Sequence | Tm (°C) | Reverse Sequence | Tm (°C) |
|---|---|---|---|---|
| | | 56.5 | CTGGACCCAGAGTGGTG | 57.6 |
| Exon 2 | ACATGCCTTTTCTGTTGTCTTC | | | |
| Exon 3 | CAACCCTTGTTTTTCTTGTTC | 54.0 | CAATGCAACCCATGGTGTC | 56.7 |
| Exon 4 | GGCTTGTGAAATCAACCTAAC | 55.9 | GAAAACTAAATGTCTGCCTC | 53.2 |
| Exon 5 | ACAGTCTGGTTTGGTAATAG | 53.2 | GACAATAACAAATTTTAAGTGG | 50.9 |
| Exon 6 | AGAGAATATTTTGCTTGCAGAG | 54.7 | GGCAAATGACAGGTGTAACAG | 57.9 |
| Exon 7 | CCTTCTCACTTCTCACGGAC | 59.4 | AAGAAATTACTCAGTTGGATAC | 52.8 |
| Exon 8 | GTGATGTGTTTAGCTGTGGT | 55.3 | GATTGAGTCTATCTTGTGGT | 53.2 |
| Exon 9 | GGGATTACAGGCATGAGCCAC | 61.8 | AGATCAGCAATGAAGCAAGTTCC | 58.9 |
| Exon 10 | TGGACAGAATTGGGAGATGAC | 57.9 | TGTGTTAAGAGGTTGGGGAG | 57.3 |
| Exon 11 | ATGATGGCTAATGCTCTCCT | 55.3 | TTCTCTGGAACTCATCTCTG | 55.3 |
| Exon 12 | CTGGTGGATTGTATTTTTGCC | 55.9 | ACAGCGAGTCTCACAAAGAAC | 57.9 |
| Exon 13 | TGTGTGTGTTTTCTCCTACT | 53.2 | TTTGTCTCTGTTCCAGGATG | 55.3 |
| Exon 14 | AGAGCAGAACGAGGTTTTATTTG | 57.1 | CACACAGAGAAAGCTTCCCAC | 59.8 |
| Exon 15 | TCTTCCGAACCTCTCCTCTC | 59.4 | CCCTCTGCAGTCCTGTCTGG | 63.5 |

Abbreviation: Tm, melting temperature.

## Supplementary Table S6. Primers for *F13A1* Promoter Region (6: 6,319,201 − 6,321,384:-1; 2 KB upstream from start codon of *F13A1*)

| Segment | position | Forward | Tm (°C) | Reverse | Tm (°C) |
|---|---|---|---|---|---|
| s1 | 6:6321519 (-2678) − 6320920 (-2079) | GGCATGCACCTGTAGTTCC | 59.1 | AACCAGTTGCTGGGAGTACC | 59.07 |
| 2 | 6:6321008 (-2344) − 6320456 (-1792) | AAACCCTCCCAGACCCTCT | 59.9 | GCAAGTGGAGCTGCCTGT | 60.1 |
| 3 | 6:6320531 (-1867) − 6319949 (-1285) | ACCTCGGTTTCCTGGTTGA | 60.5 | TGAGAAATACCGAAGGTAGGC | 58.3 |
| 4 | 6:6320031 (-1367) − 6319487 (-823) | CCCCTTAGCACTGTGTCTCC | 59.7 | GCAGGCACTGAGCCAGTTTA | 61.5 |
| 5 | 6:6319570 (-906) − 6319039 (-375) | CCCTTCATTTGGTCATTTGG | 60.2 | TGCATGTGCTGTATCTATGTTCA | 59.3 |

Abbreviation: Tm, melting temperature.

## Supplementary Table S7. Primers for Site-Directed Mutagenesis

| | Forward | Tm (°C) | Reverse | Tm (°C) |
|---|---|---|---|---|
| Lys679 Met FXIII-A | CCA ATG AAG **ATG** ATG TCC CGT GAA ATC CGG CCC AAC TCC ACC GTG | 69.5 | CAC GGT GGA GTT GGG CCG GAT TTC ACG GGA CAT **CAT** CTT CAT TGG | 67.0 |
| FXIII-A with AAAA | CTC TGT CCA TCA CAT ACA GGC AAG **CGG CCG CGG CGC** CAT CTT CAA ACT GAC CAT AGC T | 93.5 | AGC TAT GGT CAG TTT GAA GAT **GGC GCC GCG GCC G**CT TGC CTG TAT GTG ATG GAC AGA G | 93.5 |

Abbreviation: Tm, melting temperature.

## Supplementary Table S8. Primary and Secondary Antibodies

| Antibody | Product no. | Manufacturer | Concentration | Application |
|---|---|---|---|---|
| Human Integrin alpha 4/CD49d MAb (Clone 7.2R) | MAB1354 | bioTechne | 1:100 IF<br>1:1,000 WB | IF, WB |
| Mouse monoclonal [12G10] to Integrin beta 1 | NB100-63255 | bioTechne | 1:100 IF | IF |
| Rabbit polyclonal to FXIII-A | ab97636 | Abcam | 1:1,000 | WB |
| Sheep polyclonal to FXIII-A | ab 104559 | Abcam | 1:100 | IF |
| Mouse monoclonal to Collagen I | sc-293182 | Santacruz | 1:200 | WB |
| Mouse monoclonal to Collagen I | ab 90395 | Abcam | 1/2,000 | IF |
| Rabbit monoclonal [Y92] to PDGF Receptor beta | ab32570 | Abcam | 1:100 IF<br>1:5,000 WB | IF, WB |
| Rabbit polyclonal to phosphor- PDGF-Receptor β(Tyr751) | 3161 | Cell Signaling Technology | 1:1,000 | WB |
| Polyclonal rabbit IgG to p38α | AF8691 | bioTechne | 0.5μg/mL | WB |
| Mouse monoclonal to human phospho-p38α | MAB8691 | bioTechne | 0.5μg/mL | WB |
| Rabbit polyclonal antibody to Akt | 9272 | Cell Signaling Technology | 1:1,000 | WB |
| Rabbit polyclonal antibody to p-Akt(Ser473) | 9271 | Cell Signaling Technology | 1:1,000 | WB |
| Rabbit IgG antibody to LRP-6 | 2560 | Cell Signaling Technology | 1:1,000 | WB |
| Rabbit polyclonal to phosphor- LRP6(Ser 1490) antibody | 2568 | Cell Signaling Technology | 1:1,000 | WB |
| Rabbit IgG antibody to p44/42 MAPK(ERK1/2) antibody | 4695 | Cell Signaling Technology | 1:1,000 | WB |
| Rabbit IgG antibody to phosphor- p44/42 MAPK(ERK1/2)(Thr202/Tyr204) antibody | 4370 | Cell Signaling Technology | 1:1,000 | WB |
| Rabbit polyclonal to fibronectin | ab2413 | Abcam | 1:100 IF<br>1:1,000 WB | IF, WB |
| Rabbit polyclonal to GAPDH | ab9485 | Abcam | 1:2,500 | WB |
| Polyclonal Goat anti-rabbit Ig-HRP | P0448 | Dako | 1: 5,000 | WB |
| Polyclonal Goat anti-mouse Ig-HRP | P0447 | Dako | 1:2,000 | WB |
| Mouse IgGκ binding protein-HRP | sc-516102 | Santacruz | 1: 1,000 | WB |
| Donkey Anti-Rabbit IgG H&L (Alexa Fluor 647) | ab150075 | Abcam | 1:200 | IF |
| Donkey Anti-Sheep IgG H&L (Alexa Fluor; 568) | ab150177 | Abcam | 1:200 | IF |
| Goat Anti-Mouse IgG H&L (Alexa Fluor 488) | ab150113 | Abcam | 1:200 | IF |

Abbreviations: IF, immunofluorescence; HRP, horseradish peroxidase; MAPK, mitogen-activated protein kinase; PDGF, platelet-derived growth factor; WB, western blot.